

Numerical study of self-oscillations in a laser with an unstable cavity

N N Elkin, A P Napartovich

Abstract. The dynamics of oscillation in a laser with an unstable cavity is numerically simulated. The calculations are made in the nonstationary diffraction approximation taking into account the gain saturation in an active medium. The range of parameters in which stationary stable lasing is not reached was found to be considerably wider than the instability region obtained on the basis of the linear analysis of stability of stationary modes. The analysis showed the existence of a self-modulation instability that leads to the generation of a train of short sharp power peaks. The dependence of their repetition period on the gain relaxation time and the excess over the laser threshold was obtained. Doubling and quadrupling of the period of power peaks were found and the conditions providing lasing with the dynamic chaos were determined.

1. Introduction

Unstable cavities are used in high-power lasers with a large aperture for efficient selection of one transverse mode [1]. Numerical studies of the spectrum of natural modes of an unstable cavity without an active medium [1] showed that when an outcoupling mirror with sharp edges was used, modes with the lowest loss alternated with changing Fresnel cavity number $F = a^2/(\lambda L)$, where a is the radius of the outcoupling mirror; λ is the wavelength; and L is the cavity length. On the basis of these studies, practical recommendations for the choice of cavity parameters were formulated.

In particular, it is recommended, when increasing the factor M of a confocal cavity that operates on the positive branch of the stability diagram, to chose the parameters so that the equivalent Fresnel number $F_{\text{eq}} = F(M - 1)/2$ would be close to a half-integer [1]. If F_{eq} is close to an integer, two transverse modes have nearly the same loss, and a laser can simultaneous operate on both of them. Note that this is not disastrous for the laser radiation divergence because these modes insignificantly differ in divergence.

However, it is reasonable to expect that the nonlinear competition between the modes can give rise to dynamic las-

ing regimes upon stationary pumping. As shown in Ref. [2], in a cavity whose Fresnel number F_{eq} is close to the point of mode degeneracy in loss, the conditions exist when both competing modes are unstable. Stationary single-mode lasing, even at optimum equivalent Fresnel numbers, can also be destabilised by a transverse flow of an active medium in an unstable cavity [3].

It is common to study the stability of lasing, both in single-mode and in spike regimes, within the framework of the model of quantum oscillators with lumped parameters or using the expansion in a small number of modes of an empty cavity. The results obtained in this field of study are discussed in detail in monograph [4], which contains an extensive list of references. In this approach, the modes used for the expansion and their frequencies are assumed to be unchanged, whereas the structure of the total field varies in time in accordance with the dynamics of expansion coefficients.

The situation studied here relates to the case when the nonlinear mode dynamics may be strong. Because of this it is reasonable to expect the appearance of new effects that are inherent in a laser as a distributed nonlinear system. To study the lasing dynamics correctly in such cases, one should solve nonstationary equations of diffraction optics.

In this paper, we analyse, on the basis of our numerical model, the dynamics of single-mode regimes in a laser with an unstable cavity. The effects of spatial and time beatings of the fields of different modes are taken into account within the framework of the simplified model with the saturable gain. The main attention is devoted to the analysis of cavities whose Fresnel number F_{eq} is close to the point of mode degeneracy in loss.

The laser intermode beats are associated with spatial and time inhomogeneities of the electromagnetic field in a cavity containing an inertial medium. The modes excited in a real laser with an unstable cavity may be substantially different from the modes of an empty cavity because of their nonlinear interaction and the distortions caused by inhomogeneities of an active medium. All these effects are taken into account in our model.

Note that a similar numerical study of a laser as a distributed system has been earlier carried out only for semiconductor lasers [5].

2. Mathematical formulation of the model and the solution method

We restrict our analysis to two-dimensional unstable cavities formed by two cylindrical mirrors with radii of curvature R_1 and R_2 , which are positioned at the points

N N Elkin, A P Napartovich Troitsk Institute for Innovation and Fusion Research, State Scientific Centre of the Russian Federation, 142190 Troitsk, Moscow oblast, Russia

Received 11 April, 2000

Kvantovaya Elektronika 30 (12) 1065–1071 (2000)

Translated by A N Kirkin

$z = 0$ and $z = L$ on the z -axis. It is assumed that an active medium fills the layer $0 < z < L$ and occupies the whole radiation aperture in the transverse direction.

For typical conditions, the radiation inside the cavity is described by the scalar wave equation

$$E(x, z, t) = [F(x, z, t) \exp(ik_0z) + B(x, z, t) \exp(-ik_0z)] \exp(-i\omega_0 t), \quad (1)$$

where ω_0 is the carrier frequency and $k_0 = \omega_0/c$. The carrier frequency is assumed to coincide with centre of the spectral line of the laser transition. For definiteness, the double cavity length is assumed to be a multiple of the wavelength corresponding to the carrier frequency: $2k_0L = 2\pi q$, where q is an integer. For the majority of laser media, the transition width is much greater than the spectral interval between the neighbouring axial modes. Because of this, we ignore a change in the resonance refractive index. Moreover, we assume that the nonlinearity of refraction may be ignored at all.

The smooth envelopes $F(x, z, t)$ and $B(x, z, t)$ satisfy the parabolic wave equations

$$2ik_0 \left(\frac{1}{c} \frac{\partial B}{\partial t} - \frac{\partial B}{\partial z} \right) + \frac{\partial^2 B}{\partial x^2} - ik_0 g B = 0, \quad (2)$$

$$2ik_0 \left(\frac{1}{c} \frac{\partial F}{\partial t} + \frac{\partial F}{\partial z} \right) + \frac{\partial^2 F}{\partial x^2} - ik_0 g F = 0, \quad (3)$$

where g is the gain of the active medium filling the cavity.

Assuming that the mirror surfaces have high reflectivities, we can simulate the wave reflection from the mirrors by the approximate boundary conditions

$$B(x, L, t) = -F(x, L, t) C_2(x), \quad C_2(x) = \exp \frac{ik_0 x^2}{R_2} \rho_2(x), \quad (4)$$

$$F(x, 0, t) = -B(x, 0, t) C_1(x), \quad C_1(x) = \exp \frac{ik_0 x^2}{R_1} \rho_1(x). \quad (5)$$

The real factors (the reflection functions) $\rho_{1,2}(x)$ are determined by the reflectivities $r_{1,2}$ of mirror surfaces and their size (outside the mirrors, the reflection functions vanish). For instance, if the second mirror has the transverse size $2a$ and is symmetrically positioned with respect to the z -axis, then

$$\rho_2(x) = \begin{cases} r_2, & |x| \leq a, \\ 0, & |x| > a. \end{cases} \quad (6)$$

The gain $g(x, z, t)$ will be found from the equation taking into account stimulated emission and relaxation in the inverted medium:

$$\frac{\partial g}{\partial t} = \frac{g_0 - g(1 + I)}{\tau}, \quad (7)$$

where g_0 is a constant determined by the pump conditions; $I = |B|^2 + |F|^2$ is the radiation intensity averaged over the interference beats of counterpropagating waves and normalised to the saturation intensity; and τ is the relaxation time.

Generally, the initial conditions for the electromagnetic field in the cavity can be set in the form of arbitrary functions

$$B(x, z, 0) = B_0(x, z), \quad F(x, z, 0) = F_0(x, z). \quad (8)$$

We will restrict our consideration to the functions that are linear combinations of modes of the empty cavity. This simplifies the physical interpretation of calculation results. Because in many cases, the active medium before the beginning of lasing may be treated as spatially uniform, we assume that the initial distribution of the gain in (7) is equal to zero or a certain constant.

It is important for the physical interpretation of calculation results to compare the dynamic laser field with the stationary modes:

$$B(x, z, t) = B_0(x, z) \exp(-\delta t) \exp(-i\Delta\omega t), \quad (9)$$

$$F(x, z, t) = F_0(x, z) \exp(-\delta t) \exp(-i\Delta\omega t), \quad (10)$$

where δ is the damping factor and $\Delta\omega = \omega - \omega_0$ is the shift of the oscillation frequency relative to the carrier frequency. The parameters δ and $\Delta\omega$ and the stationary field distributions $B_0(x, z)$ and $F_0(x, z)$ are found from the solution of the eigenvalue problem for the operator that transforms the transverse field distribution on a cavity round trip. Let us briefly describe two typical formulations of the eigenvalue problem.

The first problem appears under the assumption of a 'frozen' medium, when the gain is not determined from Eqn (7), but is a specified function of coordinates:

$$g(x, z, t) \equiv \tilde{g}(x, z). \quad (11)$$

In this case, we have a linear eigenvalue problem for a non-Hermitian operator whose complex eigenvalue γ is related to the oscillation frequency and the damping factor by the expression

$$\gamma = \exp(-g_t L - i2\Delta k L), \quad (12)$$

where $g_t = 2\delta/c$ is the threshold gain for the lowest mode and $\Delta k = \Delta\omega/c$. The eigenvalue γ uniquely determines g_t and, therefore, the eigenmode damping. The eigenmode frequency shift relative to the carrier frequency is ambiguous:

$$\Delta k = \frac{-\arg \gamma + 2\pi n}{2L},$$

where n is the longitudinal mode index.

Here, we will study the interaction between different longitudinal modes and, therefore, set everywhere $n = 0$. The solution of a linear spectral problem allows one rigorously define the lasing threshold. If all the eigenmodes, for the given distribution $\tilde{g}(x, z)$ of the gain, satisfy the condition $|\gamma| \leq 1$, a laser operates below the threshold and no lasing can be obtained there. If at least one mode satisfies the condition $|\gamma| > 1$, its field will be enhanced until the moment when the nonlinear gain saturation, which is described by Eq. (7), manifests itself.

In this regime, which is called the above-threshold regime, various scenarios of the laser dynamics are possible. One of them is the development of the steady-state regime when the field intensity is independent of time. It follows from (7) that the gain in this case satisfies the equation

$$g = \frac{g_0}{1 + I}. \quad (13)$$

In this case, the field damping δ vanishes, and the expression for the field represents the solution of the eigenvalue problem for the operator that describes the transformation of the transverse field distribution upon a cavity round trip. One can see from (13) that the operator in this case is nonlinear.

The eigenvalue γ of the problem is related to the natural frequency by the expression

$$\gamma = \exp(-i2\Delta kL). \quad (14)$$

The resulting stationary solutions of the problem may be both stable and unstable. To determine their stability with respect to the excitation of neighbouring modes, one should freeze a medium in the solution found for of the nonlinear problem and find linear eigenmodes. If one finds that a laser is above the threshold, the solution is unstable; otherwise the solution of the nonlinear problem is stable with respect to the excitation of neighbouring modes. The numerical algorithms of the stationary problems formulated here are described in Refs [2, 6–8]. A method for the numerical solution of the basic (nonstationary) problem is described in Ref. [9].

3. Results of numerical simulation

The calculations were carried out for the following laser parameters: $L = 150$ cm; $\lambda = 1.06 \times 10^{-3}$ cm; $M = 2$; $T = 2L/c = 10^{-8}$ s. The above-threshold lasing regime was characterised by the factor $\kappa = g_0/g_t$, which specifies the excess over the threshold. Taking into account the specific features of the spatial field distribution in unstable cavities, it is sufficient to use for the variable z a grid consisting of a small number N_z of cells. The majority of calculations was made for $N_z = 4$.

In contrast, the field profile along the x -axis is strongly irregular. In the majority of calculations, we used the number of cells $N_x = 512$. To test the accuracy, some versions were recalculated using the a higher-density grids $\{N_z = 8, N_x = 512\}$ and $\{N_z = 4, N_x = 1024\}$. We will discuss the calculation accuracy below when describing the results of numerical simulation. Note that the mirror edges were not smoothed in the calculations, i. e., the reflection from a mirror was modelled using Eq. (6).

3.1. Beats of two transverse modes

In Refs [2, 10], the stability of stationary single-mode lasing with respect to the excitation of neighbouring transverse modes in a laser with a telescopic cavity was studied. It was shown that in the case of a medium with saturable gain and a cavity whose Fresnel number F_{eq} is close to the point of degeneracy of modes in loss in an empty cavity, the conditions exists when both competing modes are unstable. This instability corresponds to the approximation of the linear theory when the effect of a developing mode on the gain may be ignored.

Such conditions are realised in a leaf-shaped region on the phase plane (F_{eq}, g_0) . Its lower point has the coordinates (F_{eq}^*, g_t) , where F_{eq}^* is the equivalent Fresnel number at which the two lowest modes have the same loss. In Fig. 1, this region for $M = 2$ in the neighbourhood of the degeneracy point with

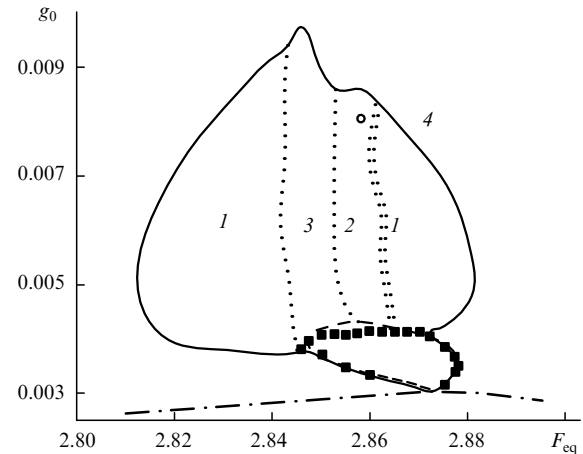


Figure 1. Boundaries of stationary-lasing stability (solid curve), linear instability (dashed curve), and the region of transverse-mode beats (squares), and the oscillation threshold (dot-and-dash curve). The dotted curves separate the regions with different types of power oscillations: the region with a periodic sequence of identical peaks (1), the region with an alternating sequence of two peaks of different height (2), and the region with a sequence of peaks that does not form a periodic structure (3). The external region 4 represents the region of stable single-mode lasing.

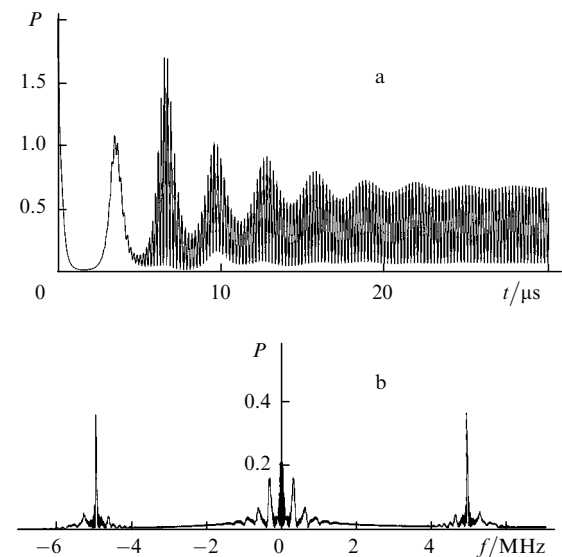


Figure 2. Transverse-mode beats at $\tau = 2.6$ μs , $F_{\text{eq}} = 2.872$, and $\kappa = 1.12$: the time dependence of power (a) and the spectrum of power oscillations (b).

$F_{\text{eq}}^* = 2.872$ is surrounded by the dashed line. The dot-and-dash curve shows the dependence of the threshold gain on F_{eq} .

It is reasonable to expect that no stationary lasing will be obtained for the points inside the region of linear instability in the nonstationary model. This statement is supported, in particular, by the calculations at the points lying inside the closed curve shown by the squares. The relaxation time τ obtained in our calculations was 2.6 μs .

The results of calculations for a typical version from a series of calculations inside the region of transverse-mode beats are presented in Fig. 2. They were obtained for the parameters $F_{\text{eq}}^* = 2.872$ and $\kappa = 1.12$. Fig. 2a presents the time dependence of the power for the wave incident on the outcoupling mirror

$$P(t) = \int_{-\infty}^{\infty} |F(x, L, t)|^2 dx.$$

The spectrum of power oscillations, i. e., the modulus of the Fourier transform of the function $P(t)$ is shown in Fig. 2b. One can clearly see the peaks, which give evidence of oscillations at a frequency of 4.9 MHz. Given the phases of eigenvalues of linear cavity modes, one can exactly determine the frequency of transverse-mode beats by the formula $\nu_b = |\arg \gamma_1 - \arg \gamma_2| / (2\pi T)$.

For two lowest modes of the empty cavity under study, the beat frequency is 5.8 MHz, which noticeably differs from the frequency of power oscillations found above. This difference is caused by the frequency shift of the lasing mode under the action of the nonlinear medium. We found from the calculation of nonlinear modes that the beat frequency of two modes with the highest Q factor was 4.9 MHz. This value virtually coincides with the frequency of laser power oscillations.

Another specific feature of the function $P(t)$ (Fig. 2) is that it has deep dips at the minima of power. This feature can be qualitatively explained in terms of linear modes whose field phase varies in time as $\sim \exp(-i\Delta\omega t)$. As shown in Ref. [11], in an empty telescopic cavity with cylindrical mirrors at the point of mode degeneracy in loss, the spatial field distributions differ from one another only insignificantly.

In the version under consideration, the nonlinear distortions of modes losses are low and, if lasing is excited on two almost identical modes, their linear combination with the coefficients $\exp(-i\Delta\omega_1 t)$ and $\exp(-i\Delta\omega_2 t)$ gives the time dependence of the form $(1 + \cos(\omega_b t))$ with the frequency $\omega_b = |\Delta\omega_1 - \Delta\omega_2|$. Note that the transverse-mode beats are modulated by a smooth oscillating envelope with a characteristic frequency of 0.3 MHz.

The formation of a stationary mode in the cavity is accompanied by relaxation oscillations, whose frequency is approximately described by the formula [4]

$$\nu_r = \frac{1}{2\pi} \left[\frac{(\kappa - 1)cg_1}{\tau} - \frac{\kappa^2}{4\tau^2} \right]^{1/2}. \quad (15)$$

The calculation by this formula gives $\nu_r = 0.326$ MHz, which suggests that the smooth oscillations in Fig. 2 represent relaxation oscillations. In the given version, the initial field was set in the form of one of the modes of the empty cavity. During the first 4 μ s, lasing was observed on this mode, and subsequently one more transverse mode was developed due to the instability. The appearance of the second mode is characterised by increasing oscillations in the plot, which correspond to transverse-mode beats.

Generally speaking, the region of beats in Fig. 1 does not coincide with the region of linear instability. The boundary of the beat region (the curves shown by squares) merges with the boundary of the region of linear instability (the dashed curve) only in the lower part; whereas in the upper part, the curves substantially differ.

3.2. Self-oscillatory lasing regimes

Outside the region of linear instability, which is bounded in Fig. 1 by the dashed curve, stationary nonlinear modes exist that are stable in the linear approximation to the excitation of other transverse modes. Our numerical calculations showed that, despite expectations, the development of lasing only sometimes leads to the formation of a

stationary nonlinear mode. The solid closed curve in Fig. 1 specifies the region where stable stationary lasing is not realised for one or another reason. Inside this region, which was obtained from the nonlinear calculations for $\tau = 2.6$ μ s, both the region of linear instability and the region of transverse-mode beatings are found, which are considerably smaller in size than the instability region. The region where stationary lasing is not realised has a rather complex structure. In addition to the aforementioned region of transverse-mode beats, several types of self-oscillatory regimes exist there, and we now turn to their description.

Consider in greater detail the dynamics of lasing for the version with parameters $F_{eq} = 2.872$ and $\kappa = 1.97$ that belong to subregion 1 consisting of two isolated parts. Figure 3a presents the time dependence of the power of the wave incident on the outcoupling mirror. After first 5 μ s of the transient process, a periodic train of identical short pulses with a high peak intensity is formed.

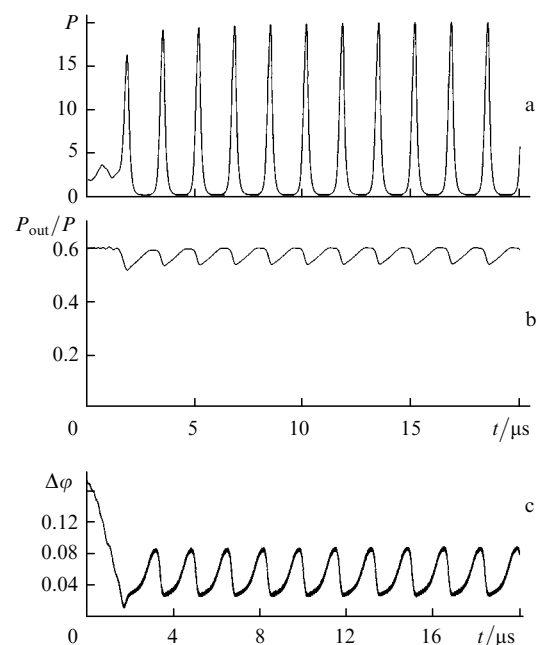


Figure 3. The regime of a periodic sequence of power peaks at $\tau = 2.6$ μ s, $F_{eq} = 2.872$, and $\kappa = 1.97$: the power of the wave incident on the outcoupling mirror (a), the portion of power contained in the output wave (the loss factor) (b); and the change in field phase (c).

It is natural that the results presented above bring up the question of the accuracy of numerical simulation. The calculation of each version of nonstationary lasing requires several tens of thousands of time steps. In this situation, it is unreal to require that the fields in the cavity be determined with a high accuracy at all moments of time. The aim of numerical simulation is to obtain a reliable qualitative picture within the framework of the given model. It is advantageous to control the calculation accuracy by one parameters or another that are of physical importance.

One of such parameters is the repetition period of the peaks shown in Fig. 3a. In our calculations, the period was 1.71 μ s for the grid $\{N_z = 4, N_x = 512\}$, 1.67 μ s for the grid $\{N_z = 8, N_x = 512\}$, and 1.79 μ s for the grid $\{N_z = 4, N_x = 1024\}$. Thus, the period obtained in the calculations on grids with an increased number of elements differs from

the period obtained on the basic calculation grid by no more than 5%, which seems to be quite satisfactory.

The spatial distribution of the field intensity depends on time weakly and, because the modes of the empty cavity have close spatial distributions, it is difficult to determine from the transverse intensity distribution which of the modes is (are) involved in lasing. One can make more definite conclusions by determining the laser radiation frequency and comparing it with the frequencies of modes of the empty cavity.

For this purpose we shall analyse the field phase at a certain point, for instance, at the centre of the outcoupling mirror. Let us introduce the notation

$$\varphi(t) = -\arg F(0, L, t).$$

In the case of stationary oscillations, $\varphi(t) = \Delta\omega t$, where $\Delta\omega$ is the shift of the mode frequency relative to the carrier frequency ω_0 . Let us determine the instantaneous frequency (more precisely, its shift relative to ω_0) by the formula $\Delta\omega = d\varphi/dt$. For convenience, we shall multiply the frequencies by T and write them in the dimensional form. For this purpose, we introduce the notation

$$\Delta\varphi(t) = T \frac{d\varphi}{dt}.$$

The quantity $\Delta\varphi(t)$ represents the phase shift produced in the time T by the current instantaneous frequency. In the linear case, $\Delta\varphi(t) = -\arg \gamma$.

Fig. 3c presents the dependence $\Delta\varphi(t)$ for the version under consideration. The frequencies of two modes with the highest Q factors of the empty cavity, measured in dimensionless units, are equal to 0.172 and -0.192 , respectively. The initial field was taken in the form of the first of these modes, which is demonstrated by the fact that $\Delta\varphi(0) = 0.172$.

In the steady-state regime, the function $\Delta\varphi(t)$ oscillates about the value $\Delta\varphi \approx 0.05$. In this version, the stable stationary nonlinear mode has a frequency of 0.036. The other (unstable) nonlinear mode has a frequency of -0.022 . Both these modes are produced by the aforementioned modes of the empty cavity. The time dependence of the frequency presented here suggests that the laser field is close to the stationary mode. However, it does not tend to it, but executes undamped self-oscillations about this mode.

Thus, self-oscillations are not related to the nonlinear interaction of different modes, but are caused by the frequency change due to the deformation of the transverse structure.

It is also interesting to find the time dependence of the loss factor $P_{\text{out}}(t)/P(t)$, where $P_{\text{out}}(t)$ is the output radiation power. Fig. 3b presents the time dependence of the loss factor. It has a periodic form, and the modulation period is the same as the period in Fig. 3a. The loss factor for the stationary nonlinear mode is 0.559. The modulation of the loss factor in the nonstationary regime is caused by the nonlinear gain saturation in a nonuniform field.

In addition to the version presented in Fig. 3, we calculated the case in which the initial field and gain distributions were taken from the corresponding stable solution of the stationary problem. At the initial stage (several microseconds long), the field in the cavity was unchanged, but later on there developed an instability because of the errors of computer simulation and the errors of the solution of the stationary problem, and this instability led to the same self-oscil-

lations as in Fig. 3. The ‘soft’ excitation of self-oscillations obtained in this way demonstrates that lasing on a stationary mode is unstable, but the instability mechanism in this case differs from the mechanism of the beats of two transverse modes considered in the previous section.

Therefore, it is reasonable to say that we have discovered a new self-oscillation instability in the numerical experiment. Its mechanism includes a frequency change depending on the field distribution and the modulation of loss because of the gain saturation. One can easily see from the comparison of Figs. 3a and 3b that a laser spike is developed at the moment of a decrease in the loss factor. In turn, the change in the loss factor may be initiated by a change in the mode frequency.

Consider the version with parameters $\kappa = 2.5$ and $F_{\text{eq}} = 2.872$. It corresponds to region 4, which lies outside the instability region for which we presented the dependences $P(t)$ and $\Delta\varphi(t)$ in Fig. 4. One can see that lasing develops according to the scenario of formation of the stationary mode. The power $P(t)$ executes damped oscillations with a period of $1 \mu\text{s}$. The period of relaxation oscillations found by formula (15) is $0.87 \mu\text{s}$, which is close to the value observed in the numerical experiment.

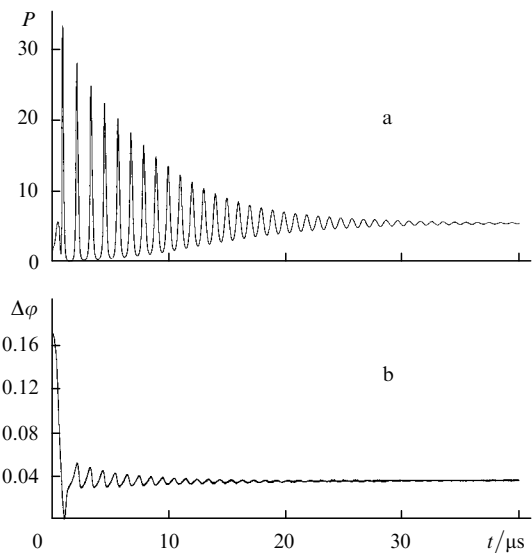


Figure 4. Formation of stationary lasing [power (a) and phase (b)] at $\tau = 2.6 \mu\text{s}$, $F_{\text{eq}} = 2.872$, and $\kappa = 2.5$.

The dependence $\Delta\varphi(t)$ tends to a constant value of 0.034. In this version, the stationary mode has a frequency of 0.0339, which is virtually coincident with the limiting value of $\Delta\varphi(t)$. Thus, we can reliably state that lasing outside the instability region is developed according to the scenario of formation of the stable stationary mode, its power executes relaxation oscillations during the mode formation, and one can estimate their period by formula (15).

Turning back to the region of self-oscillatory regimes, we shall try to find the factors determining the period of laser power oscillations. For this purpose, we made a series of calculations for $F_{\text{eq}} = 2.872$, by varying parameters κ and τ . The dependence of the oscillation period on the parameters κ and τ is presented in Fig. 5, where we compare it with the corresponding dependences for the frequency of relaxation oscillations that was calculated by formula (15).

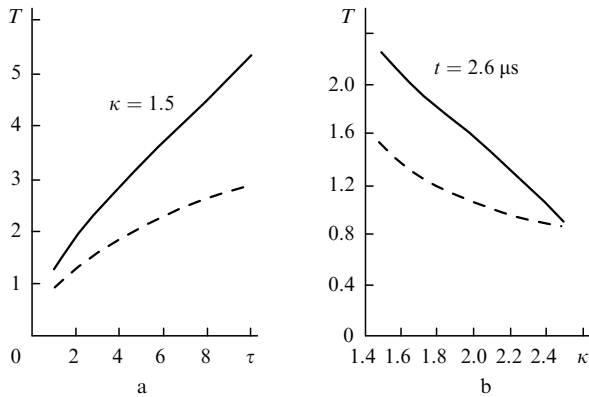


Figure 5. Dependences of the period of power oscillations (solid curves) and the period of relaxation oscillations ($1/\nu_r$) calculated by formula (15) (dashed curves) on τ (a) and κ (b) at $F_{\text{eq}} = 2.872$.

Note that the form of oscillations was similar to that shown in Fig. 3. A N Oraevskii has drawn our attention to the expression for the period of nonlinear self-oscillations

$$T_{\text{NL}} = \frac{2}{\kappa - 1} \left(\frac{2I_{\text{max}}\tau}{cg_t} \right)^{1/2}. \quad (16)$$

which was obtained in [12] (see also [4]).

To compare this dependence with the numerical results presented in Fig. 5, one should determine I_{max} . In our case, the intensity was noticeably nonuniform, both over the cross section and along the cavity. One can estimate the dependence $T_{\text{NL}}(\tau)$ by replacing the intensity by the peak intensity incident on the outcoupling mirror. The calculation by formula (16) shows that the period is almost proportional to τ , which agrees with the data of Fig. 5. This means that the real peak laser power does not change with τ (remind that the power is normalised to the saturation power, which is proportional to τ^{-1}).

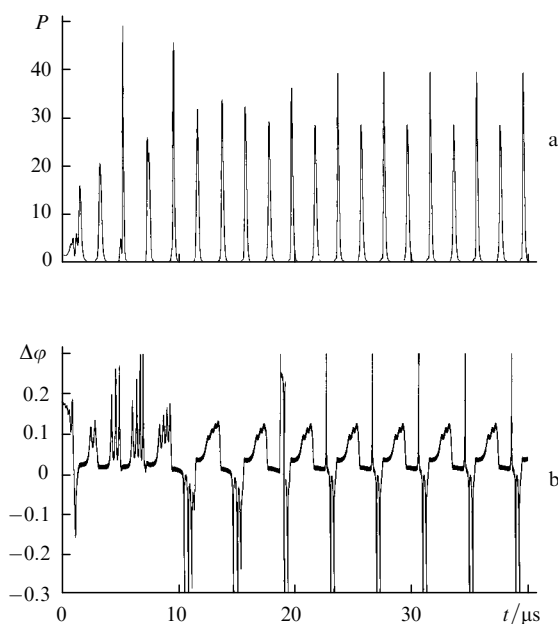


Figure 6. Formation of an alternating two-peak sequence of P (a) and $\Delta\varphi$ (b) at $\tau = 2.6 \mu\text{s}$, $F_{\text{eq}} = 2.8575$, $T > 20 \mu\text{s}$, and $\kappa = 2.03$.

Another characteristic type of self-oscillations consists in the fact that the peaks of two different heights form an alternating sequence. This phenomenon is observed in region 2 (Fig. 1) and corresponds to the period doubling, which is well known in the vibration theory. Fig. 6 presents the dependences $P(t)$ and $\Delta\varphi(t)$ illustrating (for $T > 20 \mu\text{s}$) this regime, which was obtained for $F_{\text{eq}} = 2.8575$, $\kappa = 2.03$, and $\tau = 2.6 \mu\text{s}$. Here, the oscillation picture is more complex than in the case illustrated in Figs 3 and 4, and the dependences obtained do not allow one to make a conclusion that oscillations occur on a certain definite mode. We also found the versions in which four peaks of different height formed an alternating sequence (period quadrupling). One of the versions is shown by the circle in Fig. 1.

Finally, in the region 3 in Fig. 1, we observed even more complex sequences of peaks that did not form periodic structures within the limits of the calculated time interval. One of these versions, with parameters $F_{\text{eq}} = 2.8475$, $\kappa = 2.07$, and $\tau = 2.6 \mu\text{s}$, is presented in Fig. 7. The plot of power has the form of a sequence of short sharp peaks with an aperiodic change in height. In this case, the spectrum represents a band and contains no pronounced isolated frequencies, which gives evidence of an irregular character of oscillations that may be classified as dynamic chaos.

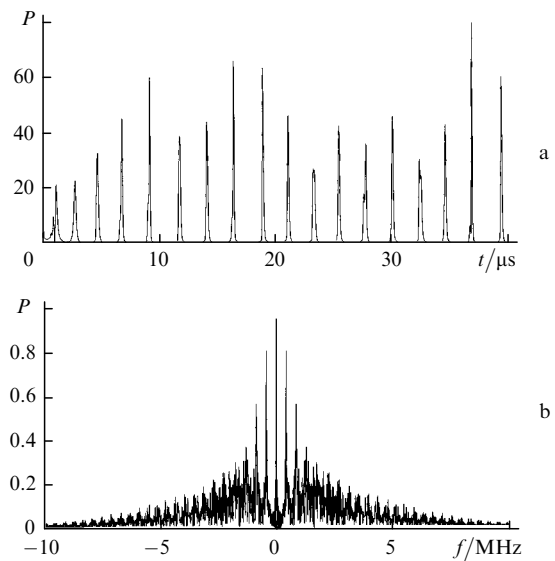


Figure 7. Irregular sequence of power peaks P (a) and its spectrum (b) at $\tau = 2.6 \mu\text{s}$, $F_{\text{eq}} = 2.8475$, and $\kappa = 2.07$.

The boundaries between the regions with definite oscillation types are shown in Fig. 1 by the dotted lines. In reality, they represent narrow layers with a very complex structure that is not shown in Fig. 1. To indicate this fact, the boundary between regions 1 and 2 is drawn by two lines. In a certain layer, whose thickness is of the order of the distance between these two lines, either an irregular sequence of peaks or a sequence with the period greater than 2 is realised.

4. Conclusions

Our comprehensive analysis of the dynamics of oscillation in a laser with an unstable cavity within the framework of the simplest model of gain saturation showed the possibility of realisation of different nonstationary lasing re-

gimes. We found a region of parameters on the plane (effective Fresnel number, excess over the lasing threshold) where undamped regular beats of the fields of two modes, regular self-oscillations changing to chaotic oscillations, and a stable stationary regime can be observed upon small deviations of these parameters.

Note that these phenomena take place in the absence of self-phase modulation, i.e., the nonlinear change in the refractive index of the medium. The oscillations are induced by a new instability mechanism, which is caused by the dependence of characteristics of a nonlinear optical mode, namely, its natural frequency and the loss factor, on the light intensity.

A N Oraevskii has drawn our attention to the paper of A F Suchkov [13], where the author numerically found self-oscillations in a simplified model of a laser with a plane-parallel cavity and an amplifying medium concentrated in a narrow near-axis region. Except for the difference in cavity types, the conditions in which these oscillations were obtained are close to the conditions analysed in our paper. However, the analysis made by A F Suchkov was restricted only to the case of total mode degeneracy in loss, and the oscillations observed there are close in nature to the mode beat that take place in the region of transverse-mode beats in Fig. 1. A detailed comparison of oscillation mechanisms is complicated by the fact that paper [13] contains only a brief description of results.

Our results show that the so-called ‘lumped’ models of lasing dynamics [4] have a limited applicability.

Acknowledgements. The authors thank A N Oraevskii for his interest in the work and valuable remarks.

References

1. Anan'ev Yu A *Opticheskie Rezonatory i Problema Raskhodimosti Lazernogo Izlucheniya* (Optical Cavities and the Divergence of Laser Radiation) (Moscow: Nauka, 1979)
2. Elkin N N *Matematicheskoe Modelirovanie* **2** (9) 133 (1990)
3. Dreizin Yu A, Dykhne A M *Pis'ma Zh. Eksp. Teor. Fiz.* **19** 718 (1974)
4. Khanin Ya I *Dinamika Kvantovykh Generatorov (Kvantovaya Radiofizika)* [Dynamics of Quantum Oscillators (Quantum Radiophysics)] (Moscow: Sov. Radio, 1975), Vol. 2
5. Adachihara H, Hess O, Abraham E, et al. *J. Opt. Soc. Am. B: Opt. Phys.* **10** 658 (1993)
6. Elkin N N, Korotkov V A, Likhanskii V V, et al. *Proc. SPIE Int. Soc. Opt. Eng.* **1031** 229 (1989)
7. Elkin N N *Matematicheskoe Modelirovanie* **2** (5) 104 (1990)
8. Elkin N N, Napartovich A P *Appl. Math. Modelling* **18** 513 (1994)
9. Elkin N N *Matematicheskoe Modelirovanie* **10** (4) 91 (1998)
10. Elkin N N, Korotkov V A, Napartovich A P, Troshchiev V E *Proc. SPIE Int. Soc. Opt. Eng.* **1224** 133 (1990)
11. Horwitz P J. *Opt. Soc. Am.* **63** 1528 (1973)
12. Belenov E M, Morozov V N, Oraevskii A N *Trudy FIAN* **52** 237 (1970)
13. Suchkov A F *Zh. Eksp. Teor. Fiz.* **49** 1495 (1965)